Instability of familial spongiform encephalopathy-related prion mutants

Yasuko Watanabe[a], Wakako Hiraoka[b], Yuhei Shimoyama[c], Motohiro Horiuchi[d], Mikinori Kuwabara[a] and Osamu Inanami[a*]

[a]Laboratory of Radiation Biology, Graduate School of Veterinary Medicine, Hokkaido University, Sapporo 060-0818, Japan

[b]Laboratory of Biophysics, School of Science and Technology, Meiji University, Kawasaki 214-8571, Japan

[c]Soft-Matter Physics Laboratory, Graduate School of Emergent Science, Muroran Institute of Technology, Muroran 050-8585, Japan

[d]Laboratory of Prion Diseases, Graduate School of Veterinary Medicine, Hokkaido University, Sapporo 060-0818, Japan

[*]Address Correspondence to: Osamu Inanami, Ph.D, Laboratory of Radiation Biology, Department of Environmental Veterinary Sciences, Graduate School of Veterinary Medicine, Hokkaido University, Kita 18-Jo Nishi 9-chome, Sapporo 060-0818, Japan. Fax: +81-11-706-7373; E-mail: inanami@vetmed.hokudai.ac.jp

Abstract

We examined the influence of D177N (D178N in humans) mutation on the conformational stability of the S2 region of moPrP^{C} with varying pHs by using the SDSL-ESR technique. The ESR spectrum of D177N at pH 7.5 was narrower than that of Y161R1, referred to as WT*. The ESR spectrum of D177N did not change when pH in the solution decreased to pH 4.0. Our results suggested that the disappearance of a salt bridge (D177-R163) induced the increase in the instability of S2 region. Moreover, the line shape of the ESR spectrum obtained from H176S neighboring the salt bridge linked to the S2 region was similar to D177N. These results indicate that the protonation of H176 is strongly associated with the stability of S2 region. These findings are important for understanding the mechanism by which the disruption of the salt bridge in the S2 region forms the pathogenic PrP^{Sc} structure in hereditary prion disease.

Keyword: prion protein; SDSL; ESR; salt bridge; pH-sensitivity; D178N; conformational stability; histidine residue; familial spongiform encephalopathy; conformational transition

Introduction

Transmissible spongiform encephalopathys (TSEs), or prion diseases, are a group of fatal neurodegenerative disorders including Creutzfeldt-Jacob disease (CJD), Gerstmann-Sträusler-Scheinker (GSS) syndrome and fatal familial insomnia (FFI) in humans, scrapie in sheep and bovine spongiform encephalopathy in cattle [1]. Though the precise mechanism and parameters of the conversion from the normal cellular prion protein (PrP^{C}) to the abnormal (scrapie-like and β-sheet-rich) form of prion protein (PrP^{Sc}) is still unknown, the accumulation of PrP^{Sc} in endosomes, the main intracellular acidic organelles, indicates that the process of conversion from PrP^{C} to PrP^{Sc} requires physiological acidic pH conditions [2-4].

The inherited prion diseases associated with mutations in the prion protein (*PRNP*) gene coding for PrP fall into three major groups: CJD, GSS syndrome and FFI [5]. Despite their phenotypic differences, FFI and one familial type of CJD (CJD_{178}) are both linked to a single mutation of *PRNP* at codon 178 resulting in the substitution of asparagine for aspartic acid (D178N) [6]. NMR data have revealed that a residue of Asp 178 (D178) forms a salt bridge with Arg 164 (R164), which holds the β-sheet against Helix2 [7]. Moreover, the Molecular dynamics (MD) simulations indicate that the electrostatic interaction between D178 and R164 plays an important role in the dynamic stability of PrP^{C} [8]. Thus, it was proposed that the neutralization of D178 at low pH removes interactions that inhibit a structural change at neutral pH. In addition, His 187 (H187) has also been reported to be involved into a pathogenic mutation associated with GSS syndrome (H187R), which implies a positively charged residue in position 187, analogous to H187 protonation [9, 10]. A recent study suggested that the breaking of the salt bridge between Glu 195 and Arg 156 induced by the protonation of H187 at acidic pH was the key event underlying the extension of the S2

region [11]. However, there is no experimental evidence that these amino acids are involved in the structure of PrP^C such as the high flexibility of the S2 region.

Recently, to obtain experimental information about the pH-induced conformational changes, we employed cysteine-scanning site-directed spin labeling (SDSL) combined with electron spin resonance spectroscopy (ESR) and analyzed the pH-induced mobility changes in one α-helix (Helix1) and two β-sheets (Sheet1 and Sheet2) of mouse PrP^C ($moPrP^C$) [12, 13]. Our experimental data clearly demonstrated the presence of three pH-sensitive sites in $moPrP^C$, *i.e.*, (1) the N-terminal tertiary contact site of Helix1 (H1), (2) the C-terminal end of H1 and (3) the Sheet2 (S2) region [13]. At low pH, a study using MD simulation showed loosening of the tertiary structure, extension of the S2 region and gain of an extended secondary structure in the N-terminal region followed by a misfolded intermediate rich in a β-like structure and a trimetric representation of a PrP^{Sc} protofibril [14]. In addition, high resolution NMR also suggested that the residues at the C-terminal end of H1 and β-strand2 were involved in the "starting point" of pH-induced unfolding and implicated in endosomic PrP^C to PrP^{Sc} conformational transition resulting in TSEs [15]. Therefore, elucidation of how the pH-induced local mobility change correlated with the mechanism of the extension of the S2 region should provide important clues regarding the molecular basis of prion diseases.

In the present study, we examined the influence of mutations, D177N (D178N in humans) and H186S (H187S in humans), on the conformational stability of the S2 region of $moPrP^C$ at various pHs. For this purpose, we employed the SDSL-ESR method, since SDSL-ESR has been proven to be a powerful tool to monitor the structure and dynamics of proteins, which are impossible to obtain by NMR and X-ray crystallographic methods [12, 13, 16]. In our SDSL-ESR technique, the nitroxide side chain (R1) derived from (1-Oxyl-2,2,5,5-tetramethylpyrroline-3-methyl)methane thiosulfonate (MTSSL) was

introduced into a Tyr 161 (Y161) residue substituted for a cysteine residue by site-directed mutagenesis (Fig. 1A).

Materials and Methods

Materials. (1-Oxyl-2,2,5,5-tetramethylpyrroline-3-methyl)methane thiosulfonate (MTSSL) was purchased from Toronto Research Chemicals (ON, Canada). 2-[4-(2-hydroxyethyl)-1-piperazinyl]ethanesulfonic acid (HEPES) and 2-morpholinoethanesulfonic acid, monohydrate (MES) were from Dojindo, Lab. (Kumamoto, Japan). The Protein Assay Lowry Kit was from Nacalai Tesque, Inc. (Kyoto, Japan). Other reagents were from Wako Pure Chemical, Co. (Tokyo, Japan).

Construction, Expression, Purification and Spin-Labeling of recombinant moPrP^C mutants.

These experimental procedures were based on those described previously [12, 13]. To study the influences of amino acid residues Asp 177 and His 186 on the conformational stability of the S2 region around Y161R1, two plasmids containing double mutations, Y161C/D177N and Y161C/H186S, were constructed using this Y161C mutant as a template (Fig. 1B). In addition, we also created a plasmid encoding Y161C/H176S, to explore the effect of the positive charge of His 176 neighboring the salt bridge, D177-R164, on the structural stability of the S2 region. All moPrP^C mutants (Y161C, Y161C/D177N, Y161C/H186S and Y161C/H176S) were generated by the PCR-based site-directed mutagenesis method and confirmed their change using a CEQ8800 automated sequencer (Beckman Coulter, Inc.). Figure 1B shows the positions of α-carbons of D177, H186, H176 (Yellow) and Y161R1 (red) on the 3D structure in the carboxy-terminal domain of

moPrP$_{(121\text{-}231)}$ as reported by Hornemann *et al.* (Potein Data Bank entry 1AG2) [17]. The expression and purification of recombinant moPrP^{C} mutants were carried out as described previously [12, 13]. To label the moPrP^{C} mutants with MTSSL, a 10-fold molar excess of MTSSL was added to each protein and incubated overnight in the dark at 4^{o}C. The free MTSSL was removed from the protein using a microdialyzer (Nippon Genetics).

ESR spectroscopy. Details of the ESR spectroscopy methods have been published elsewhere [12, 13]. The pH change of the sample solution was carried out by dialysis of the sample against eight buffers with various pH conditions from 4.0 to 7.5: 10 mM acetate buffer (pH 4.0, pH 4.5 and pH 5.0), 10 mM MES buffer (pH 5.5, pH 6.0 and pH 6.5) and 10 mM HEPES buffer (pH 7.0 and pH 7.5). ESR spectra were recorded in a quartz flat cell (RST-DVT05; 50 mm x 4.7 mm x 0.3 mm, Radical Research) for spin-labeled samples of 20 μM moPrP^{C} using a JEOL-RE X-band spectrometer (JEOL) with a cylindrical TE011 mode cavity (JEOL). All ESR spectra were obtained at 10^{o}C, controlled by a temperature controller (ES-DVT4, JEOL), under the following conditions: 5 mW incident microwave power, 100 kHz modulation frequency, 0.2 mT field modulation amplitude and 15 mT scan range. The $1/\delta H_0$ of the central component (M_I=0: ^{14}N hyperfine) in the ESR spectrum of spin-labeled moPrP^{C} was employed as a mobility parameter and was further analyzed using a Win-Rad Radical Analyzer System (Radical Research). To analyze the stability of the S2 region in moPrP^{C} mutants, we further measured the intensities of immobile (Im) and mobile (M) nitroxide probes in the low field component (M_I=+1) in each ESR spectrum.

Results and discussion

pH-induced conformational changes of the S2 region in moPrP^C

Many studies have demonstrated the relationship between the conversion from PrP^C to PrP^{Sc} and the pH in intracellular acidic compartments such as endosomes [2-4]. In a previous study, we also analyzed the pH-induced conformational changes in moPrP^C using SDSL-ESR and provided experimental evidence for three pH-sensitive sites in the C-terminal region of moPrP^C [12, 13]. In particular, the Y161 in the N-terminal side of S2 region was identified as one of the highly sensitive site for pH change [13]. To obtain further information on the pH-sensitivity of this site, we investigated the pH-induced mobility changes of Y161R1 under various pH conditions from 4.0 to 7.5. In the present experiments, Y161R1 (moPrP^C containing a single spin label at site 161 with no additional mutations) was used for examination of the stability of the S2 region in moPrP^C and was referred to as WT*. The ESR spectrum of WT* observed at pH 7.5 showed a line broadening signal due to a major immobile component (M) with a minor mobile component (Im) (Fig. 2A). When the pH in the solution decreased from 7.5 to 4.0, the intensity of the mobile component increased relatively. To obtain detailed information about pH sensitivity, we measured $1/\delta H_0$ in ESR spectrum under various pH conditions from 7.5 to 4.0. The values of $1/\delta H_0$ obtained from the ESR spectra at pH 7.5, pH 7.0 and pH 6.5 were approximately 1.66, 1.70 and 1.72, respectively, indicating that the nitroxide probes were strongly immobilized (Fig. 2B). In contrast, the $1/\delta H_0$ from the ESR spectra when the pH in the solution changed from 6.0 to 4.0 increased abruptly from approximately 1.84 to 2.11. These pH-dependent changes of $1/\delta H_0$ from ESR spectra were observed when the pH in the solution decreased to near pH 6.5 or less. Thus it was considered that the pH-dependent mobility change in the S2 region resulted in conformational transition.

Since the pH-dependent conformational change from a rigid to a flexible structure in

the S2 region was clearly observed, we next examined whether isosbestic points were present in the ESR spectral changes induced by the decrease of pH. We prepared absorption spectra through integration of the first derivative spectrum in WT* at each pH from 7.5 to 4.0. In the superimposed spectra, six points that did not change during pH change were observed (Fig. 3C, black arrows). This observation indicated the presence of isosbestic points, suggesting that the conformational transition from a mobile structure to an immobile structure in the S2 region occurred at around pH 6.5. These findings indicated that the conformational transition occurred at between pH 6.5 and pH 6.0. These observations are the first evidence for structural instability in the S2 region in response to pH, which was assumed based on MD simulations [14].

Influence of the pathogenic mutations on the conformational stability of the S2 region with varying pH

Recently, MD simulation has shown that the mutation of Asp to Asn at position 178 plays an important role in the conformational conversion to β-sheet-rich PrP [18]. Linkages between familial prion diseases and mutations in the gene encoding human prion protein were reported and over 20 such mutations have been shown to date to segregate familial CJD, GSS and FFI [1, 19, 20]. The D178N mutation is one of the most intriguing disease-related mutations and leads to different phenotypes of human prion disease depending upon the polymorphism at position 129. The D178N mutant with methionine at 129 is associated with FFI, whereas the same mutant with valine at 129 correlates with hereditary CJD [6]. It was reported that the D178 side chain is involved in a salt bridge with R164, connecting Helix2 with the β-sheet [8, 21]. These reports led us to speculate that the D178N mutation induces a flexible structure of Helix2 and the β-sheet by disruption of a salt bridge with R164. To

clarify whether the mutations of D177 (D178 in humans) were actually associated with pH-dependent conformational changes in the S2 region, we measured the effects of pH changes on ESR spectrum of D177N. The ESR spectrum of D177N at pH 7.5 was narrower than that of WT* (Fig. 3A). The ESR spectrum of D177N did not change when the pH in the solution decreased from 7.5 to 4.0. Figure 3B shows a summary of the stability of the S2 region in all mutants. We measured the intensities of immobile (Im) and mobile (M) nitroxide probes in the low field component (M_I=+1) and calculated the Im/M ratios at pH 7.5 and pH 4.0 for each ESR signal. At pH 7.5, the Im/M ratios of WT* were approximately 1.39. However, when the pH in the solution changed from 7.5 to 4.0, the Im/M ratios of WT* significantly decreased to 0.50. On the other hand, the Im/M ratios of D177N at pH 7.5 were approximately 0.39, significantly lower than that of WT*. Moreover, pH-dependent changes in the Im/M ratio were not observed for D177N. These results suggested that the structure around S2 of the PrP^C mutant with disappearance of this salt bridge was a flexible conformation, which was similar to that of WT* in the acidic condition. If the exposure of PrP^C to acidic conditions in endosomes is accepted as a key factor in the conversion to PrP^{Sc}, the unusual flexible structure of S2 of the D177N mutant at neutral pH may induce instability prone to pathogenic conversion.

Previous experiments using ^{2}H-NMR spectroscopy have shown that the pK_a values of glutamic acid at 22 and asparagic acid at 23 on $A\beta_{(1-40)}$ amyloid peptide are approximately 4.2-4.3, whereas the pK_a values of histidine at 13 and histidine at 14 are approximately 6.2 [22]. Analysis of Cu, Zn-superoxide dismutase showed that the pK_a value of the C-terminal histidine was 6.73 [23]. Since our data showed the conformational transition of WT* started from pH 6.5 (Fig. 2B and 2C), which was close to the pK_a of the histidine residue but not that of the asparagic acid residue, and the salt bridge (D177-R163) was essential for this

pH-induced conformational transition in the S2 region of WT* as mentioned above, the histidine residue neighboring at the S2 region appeared to interfere with the interaction in the salt bridge (D177-R163). Therefore, we selected His 176 neighboring salt bridge D177-R163 and measured the ESR spectra of the H176S mutant. The line shape of the ESR spectrum obtained from H176S at pH 7.5 was narrower than that of WT* and the spectral change of H176S was small, when the pH in the solution decreased from 7.5 to 4.0 (Fig. 3A). The behavior of pH-dependent-spectral changes of H176S seemed to be close to that of D177N, rather than those of WT*, as indicated by the Im/M ratio (Fig. 3B). These results indicated that the H176 was strongly associated with the stability of S2 regions, although this histidine residue (human 177) was reported to have little effect on the overall spatial arrangement of PrP in an MD simulation study [11].

His 187 is reported to be involved in a pathogenic mutation associated with GSS syndrome (H187R) [9, 10]. A recent study indicated that the breaking of the salt bridge (E195-R156) induced by the protonation of H187 at acidic pH was the key event underlying the extension of the S2 region [11]. However, in the present study, there were no differences in either the line shapes or the value of $1/\delta H_0$ from the ESR spectra of WT* and H186S at pH 7.5 (Fig. 3A). Furthermore, the ESR spectrum of H186S became narrower when pH was decreased from 7.5 to 4.0. This pH-dependent change in the line shape and Im/M ratio of H186S was quite similar to that of WT* (Fig. 3A and 3B). These result indicated that H186 was not involved in the pH-dependent instability in the S2 region. In humans, the trigger of pH-dependent conformational changes of GSS syndrome (H187R) may be different from those of FFI and CJD_{178} with point mutation of D178. Furthermore, we examined the conformational stability of the S2 region in the Q167R mutant, which acts as a dominant-negative, an inhibitory mutant against PrP^{Sc} formation (neighboring the S2 region)

[24]. The pH-dependent mobility change in Q168R was also similar to WT* and H186S (data not shown). These results indicated that the conversion from PrP^{C} to PrP^{Sc} may be affected by several mechanisms of conformational change, including pH-dependent instability in the S2 region.

In conclusion, the present cysteine-scanning SDSL-ESR study for full-length recombinant $moPrP^{C}$ provided experimental evidence that amino acid residues D177 and H176, but not H186, were important in the pH-induced conformational instability of the S2 region. In the D177N mutant, the mobility of the S2 region at natural pH was significantly higher than that in WT* and was similar to that in WT* at acidic pH. Moreover, the conformational transition of the S2 region started from pH 6.5, which was close to the pK_a of the histidine residue and the protonation of H176 was strongly associated with the stability of S2 regions. These findings appear to be essential for understanding the mechanism by which the disruption of the salt bridge in the S2 region forms the pathogenic PrP^{Sc} structure in hereditary prion diseases.

Acknowledgments

We thank H. Tamayama and Y. Otoshima for ESR spectroscopy. This work was supported, in part, by Grants-in-Aid for Basic Scientific Research from the Ministry of Education, Culture, Sports, Science and Technology of Japan (No. 17380178 and No. 18658118 [O.I.] and No. 17580275 and No. 17658126 [M.K.]), by Research Grants from the Program for the Center of Excellence of Zoonosis Control, Sapporo 060-0818, Japan [Y.W., O.I., M.H.] and CREST-JST, Multi-Quantum Coherence ESR Project, Muroran 050-8585, Japan [Y.S.].

References

[1] S.B. Prusiner, Prions, Proc. Natl. Acad. Sci. USA 95 (1998) 13363-13383.

[2] S. Hornemann, R. Glockshuber, A scrapie-like unfolding intermediate of the prion protein domain PrP(121-231) induced by acidic pH, Proc. Natl. Acad. Sci. USA 95 (1998) 6010-6014.

[3] W.-Q. Zou, N.R. Cashman, Acidic pH and detergents enhance *in vitro* conversion of human, brain PrP^{C} to a PrP^{Sc}-like form, J. Biol. Chem. 277 (2002) 43942-43947.

[4] D.A. Kocisko, S.A. Priola, G.J. Raymond, B. Chesebro, P.T. Lansbury Jr., B. Caughey, Species specificity in the cell-free conversion of prion protein to protease-resistant forms: a model for the scrapie species barrier, Proc. Natl. Acad. Sci. USA 92 (1995) 3923-3927.

[5] P. Parchi, P. Gambetti, Human prion diseases, Curr. Opin. Neurol. 8 (1995) 286-293.

[6] L. G. Goldfarb, R.B. Petersen, M. Tabaton, P. Brown, A.C. LeBlanc, P. Montagna, P. Cortelli, J. Julien, C. Vital, W.W. Pendelbury, M. Haltia, P.R. Wills, J.J. Hauw, P.E. McKeever, L. Monari, B. Schrank, G.D. Swergold, L. Autilio-Gambetti, D.C. Gajdusek, E. Lugaresi, P. Gambetti, Fatal familial insomnia and familial Creutzfeldt-Jakob disease: disease phenotype determined by a DNA polymorphism, Science 258 (1992) 806-808.

[7] R. Riek, G. Wider, M. Billeter, S. Hornemann, R. Glockshuber, K. Wüthrich, Prion protein NMR structure and familial human spongiform encephalopathies, Proc. Natl. Acad. Sci. USA 95 (1998) 11667-11672.

[8] J. Zuegg, J.E. Gready, Molecular dynamics simulations of human prion protein: importance of correct treatment of electrostatic interactions, Biochemistry 38 (1999) 13862-13876.

[9] L. Cervenakova, C. Buetefisch, H.S. Lee, I. Taller, G. Stone, C.J. Gibbs Jr, P. Brown, M. Hallett, L.G. Goldfarb, Novel *PRNP* sequence variant associated with familial encephalopathy, Am. J. Med. Genet. 88 (1999), 653-656.

[10] C.M. Bütefisch, P. Gambetti, L. Cervenakova, K.-Y. Park, M. Hallett, L.G. Goldfarb, Inherited prion encephalopathy associated with the novel *PRNP* H187R mutation, Neurology 55 (2000) 517-522.

[11] E. Langella, R. Improta, V. Barone, Checking the pH-induced conformational transition of prion protein by molecular dynamics simulations: effect of protonation of histidine residues, Biophys. J. 87 (2004) 3623-3632.

[12] O, Inanami, S. Hashida, D. Iizuka, M. Horiuchi, W. Hiraoka, Y. Shimoyama, H. Nakamura, F. Inagaki, M. Kuwabara, Conformational change in full-length mouse prion: a site-directed spin-labeling study. Biochem. Biophys. Res. Commun. 335 (2005) 785-792.

[13] Y. Watanabe, O. Inanami, M. Horiuchi, W. Hiraoka, Y. Shimoyama, F. Inagaki, M. Kuwabara, Identification of pH-sensitive regions in the mouse prion by the cysteine-scanning spin-labeling ESR technique. Biochem. Biophys. Res. Commun. 350 (2006) 549-556.

[14] M.L. DeMarco, V. Daggett, Local environmental effects on the structure of the prion protein, C. R. Biol. 28 (2005) 847-862.

[15] L. Calzolai, R. Zahn, Influence of pH on NMR structure and stability of the human prion protein globular domain, J. Biol. Chem. 278 (2003) 35592-35596.

[16] W.L. Hubbell, H.S. Mchaourab, C. Altenbach, M.A. Lietzow, Watching proteins move using site-directed spin labeling, Structure 4 (1996) 779-783.

[17] S. Hornemann, C. Korth, B. Oesch, R. Rieka, G. Widera, K. Wüthrich, R. Glockshubera, Recombinant full-length murine prion protein, mPrP(23-231): purification and

spectroscopic characterization, FEBS Lett. 413 (1997) 277-281.

[18] A.C. Apetri, D.L. Vanik, W.K. Surewicz, Polymorphism at residue 129 modulates the conformational conversion of the D178N variant of human prion protein 90-231 Biochemistry 44 (2005) 15880-15888.

[19] P. Gambetti, Q. Kong, W. Zou, P. Parchi, S.G. Chen, Sporadic and familial CJD: classification and characterization, Br. Med. Bull. 66 (2003) 213-239.

[20] J. Collinge, Prion diseases of humans and animals: Their causes and molecular basis, Annu. Rev. Neurosci. 24 (2001) 519-550.

[21] J. Gsponer, P. Ferrara, A. Caflisch, Flexibility of the murine prion protein and its Asp178Asn mutant investigated by molecular dynamics simulations, J. Mol. Graph. Model 20 (2001) 169-182.

[22] Z. Zhang, J. P. Lee, Selectively ^{2}H-labeled Glu/Asp: application to pKa measurements in Aβ amyloid peptide, J. Peptide Res. 55 (2000) 1-6.

[23] A. Myari, G. Malandrinos, Y. Deligiannakis, J.C. Plakatouras, N. Hadjiliadis, Z. Nagy, I. Sovago, Interaction of Cu(2+) with His-Val-His and of Zn(2+) with His-Val-Gly-Asp, two peptides surrounding metal ions in Cu,Zn-superoxide dismutase enzyme, J. Inorg. Biochem. 85 (2001) 253-261.

[24] V. Perrier, K. Kaneko, J. Safar, J. Vergara, P. Tremblay, S.J. DeArmond, F.E. Cohen, S.B. Prusiner, A.C. Wallace, Dominant-negative inhibition of prion replication in transgenic mice, Proc. Natl. Acad. Sci. USA 99 (2002) 13079-13084.

Legends to figures

Figure 1 A schematic diagram of the site-directed spin labeling (SDSL) technique and the mutation site for SDSL-ESR on the 3D structure of $moPrP^C$.

(A) The reaction of the methanethiosulfonate spin-labeling reagent with the cysteine residue generates the nitroxide side chain (R1) on $moPrP^C$. (B) The carboxy-terminal domain of $moPrP_{(121-231)}$ and the mutation site for SDSL-ESR. Four α-carbons indicate the positions of D177, H186, H176 (Yellow) and Y161R1 (red) in the pH-sensitive S2 region. These α-carbons were superimposed on the 3D structure of moPrP reported in an NMR study (PDB entry 1AG2, ref. 17).

Figure 2 The effect of pH on the ESR-spectra from the WT* mutant.

(A) ESR spectra obtained from the WT* mutant at pH 7.5 and pH 4.0 were recorded using an X-band ESR spectrometer at 10^oC. The ESR spectrum at pH 7.5 showed a line broadening signal due to a major immobile component (Im, black arrow in M_I=+1) with a minor mobile component (M, white arrow in M_I=+1). (B) The changes of $1/\delta H_0$ from ESR spectra at various pHs from 7.5 to 4.0. The value of $1/\delta H$ obtained from the peak-to-peak central component (M_I=0) in each ESR is plotted. It is considered that the pH-dependent mobility change in the S2 region results in conformational transition. (C) The absorption spectra obtained by integration of first derivative spectra in WT* at pH 7.5 (black line), pH 6.5 (blue line), pH 5.0 (violet line) and pH 4.0 (red line) are superimposed. Six black arrows show the isosbestic points that did not change during pH change.

Figure 3 The roles of amino acid residues D177, H176 and H186, in the pH-dependent conformational changes in the S2 region.

(A) The ESR spectra of the WT*, D177N, H186S and H176S mutants were obtained at pH 7.5 and pH 4.0. The line shapes of spectra were obtained at pH 7.5 (black line) and pH 4.0 (red line). The immobile component and mobile component are indicated by the black arrow and white arrow in the low field component (M_I=+1), respectively. (B) The stability of the S2 region in each moPrP^C mutants. The intensities of immobile and mobile nitroxide probes obtained from ESR spectra were measured and the ratios of Im/M were calculated.

Figure

Figure 1

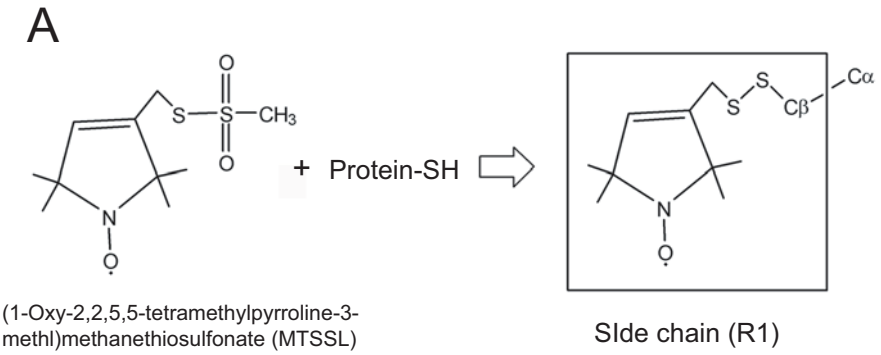

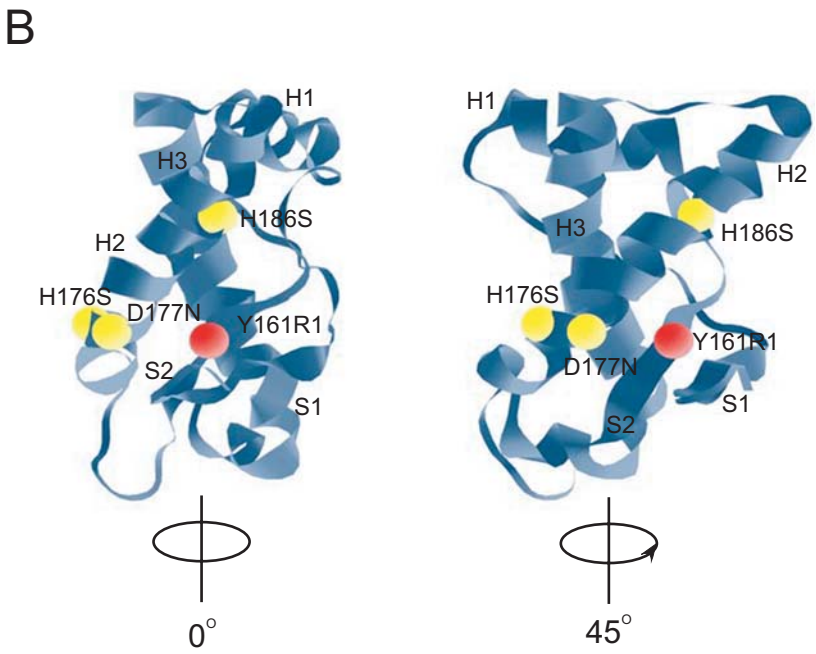

Figure 2

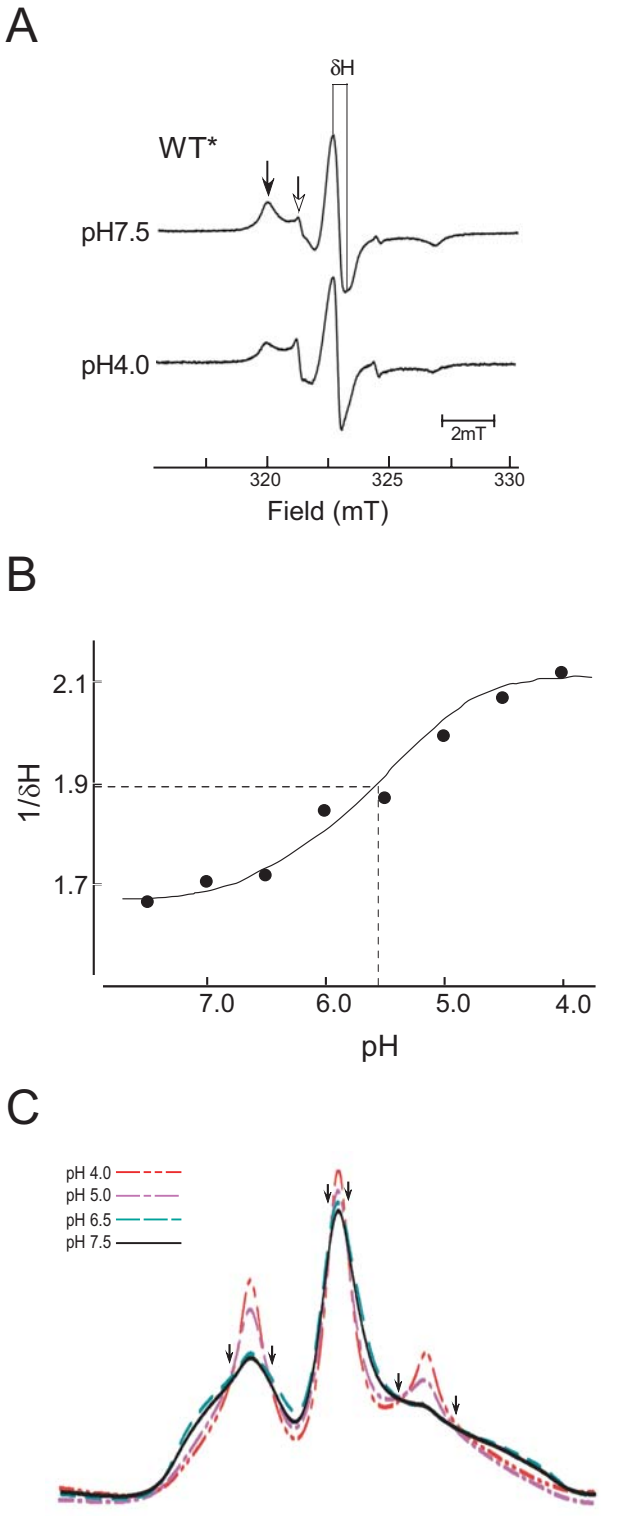
A
δH
WT*
pH7.5
pH4.0
2mT
320
325
330
Field (mT)
B
2.1
1.9
1.7
1/δH
7.0
6.0
5.0
4.0
pH
C
pH 4.0
pH 5.0
pH 6.5
pH 7.5

Figure

Figure 3